Absolute Conformations of the (−)-[9](2,5)Pyridinophane Molecule

by **Maxim Fedorovsky**[a]), **Hans Gerlach**[b]), and **Werner Hug***[a])

[a]) Department of Chemistry, University of Fribourg, Chemin du Musée 9, CH-1700 Fribourg
[b]) Department of Chemistry, University of Bayreuth, D-95440 Bayreuth

[9](2,5)Pyridinophane was first synthesized, and its enantiomers were separated, more than 40 years ago, but the molecule's absolute conformations could not be determined up to now. We show here, by the comparison of measured and computed vibrational optical activity (VOA), that the *CIP* descriptor (*P)* applies to the (−)-enantiomer. This assignment is based on the VOA of bands from vibrations localized on the pyridine ring bent by the tense $(CH_2)_9$ chain extending from position 2 to 5. The VOA of vibrations localized on the chain is in agreement with this assignment. Its behavior differs from the VOA of the bent pyridine ring, and conclusions drawn from the chain's VOA alone would not be sufficient, because the close-to-enantiomorphic geometries of the chain present in some of the 14 conformers of (−)-[9](2,5)pyridinophane lead to VOA with an opposite sign. Understanding of how VOA is generated is crucial for the unambiguous assignment of the molecule's absolute conformations.

Introduction. – [9](2,5)Pyridinophane is a simple ansa compound that was first synthesized more than 40 years ago [1]. The successful isolation of the (+)-enantiomer evidenced that the molecule exists in two stable enantiomorphic forms. Despite of (+)-[9](2,5)pyridinophane being a stable, well characterized compound, its absolute conformation could up to now not be determined, neither by chemical means, nor by electronic optical activity, nor by anomalous X-ray scattering[1]).

The successful determination, by *Raman* optical activity (ROA), of the absolute configuration of a molecule as subtly chiral as (*R*)-[$^2H_1$, $^2H_2$, $^2H_3$]neopentane [2] suggested vibrational optical activity (VOA) as the method of choice for solving the problem of the absolute conformation of pyridinophanes by a modern spectroscopic and computational approach. With some of the original racemic [9](2,5)pyridinophane still available, the separation of the enantiomers was once more undertaken (see *Exper. Part*). Here, we report the successful determination of the absolute conformations of the (−)-enantiomer of [9](2,5)pyridinophane by the comparison of its measured and computed ROA and vibrational circular dichroism (VCD) spectra.

The Structure of Conformers. – Our calculations yield 28 stable conformers for the [9](2,5)pyridinophane molecule. They fall into two enantiomorphic sets corresponding

[1]) Salts obtained with strong acids, such as HBr, from the weakly basic pyridinophane could not be crystallized, even under anhydrous conditions, and the (+)-2,2′-dihydroxy-1,1′-dinaphtyl-3,3′-dicarboxylic acid used for the optical resolution yielded polycrystalline material, unsuitable for X-ray crystallography. Attempts by several groups at the theoretical interpretation of the electronic circular dichroism [1] proved unsuccessful and remained unpublished.

to (+)- and (−)-[9](2,5)pyridinophane, for which it was found that they do not undergo interconversion up to a temperature of 250° [1]. The steric interaction of the pyridine ring with the molecule's nine-membered CH_2 chain is thus sufficient to block the rotation of the ring which would otherwise lead to the interconversion of sets. The separate signals observed in the ^{1}H-NMR spectrum for the two H-atoms of the CH_2 groups concur with this [1].

All conformers contain the common, inherently chiral helical unit of the four consecutive atoms C(2′), C(1′), C(2), and N(1), with the N-atom having the highest priority in the molecule. They define a torsion angle with a positive algebraic sign [3] for the (*P*)- and a negative sign for the (*M*)-set, where (*P*) and (*M*) are the *Cahn–Ingold–Prelog* (CIP) descriptors for a molecule's sense of chirality [4]. As it will turn out, (−)-[9](2,5)pyridinophane measured in this work corresponds to the (*P*)-set illustrated in *Fig. 1* by some of its prominent members.

The structures of the 14 conformers of either enantiomorphic set can be thought of as obtained by attaching five different geometrical arrangements of the $(CH_2)_9$ chain to the pyridine ring. One such arrangement of the chain has C_2-symmetry, two have C_s-symmetry, and two further ones have no symmetry at all. Each of the chains with no symmetry has two enantiomorphic forms, the two ends of which can be attached to the pyridine ring either from C(2) to C(5) or from C(5) to C(2), resulting in eight distinguishable conformers. Each of the two C_s-symmetric chains can likewise be fixed in two orientations to the ring, yielding another four conformers. Attaching the ends of the C_2 -symmetric chain to the ring from C(2) to C(5) or from C(5) to C(2) makes no difference as the chain's C_2-axis is perpendicular to the plane of the pyridine ring, and the two enantiomorphic forms of the chain, therefore, lead to two conformers only. Mirroring the resulting 14 structures in space yields the enantiomorphic set.

Minimizing the energies of these idealized raw structures of [9](2,5)pyridinophane does modify the geometry of the chain, and the asymmetry introduced by the presence of a N-atom in the aromatic ring is a sufficient perturbation so that the initial precise C_2- or C_s-symmetry imposed onto the $(CH_2)_9$ chain is lost, but the resulting conformers remain easily recognizable as structures obtained in the above described way.

For the sake of clarity, we will limit the further discussion to the main conformers of the (*P*)-set of [9](2,5)pyridinophane depicted in *Fig. 1*. They make up 93% of the equilibrium mixture of the (−)-enantiomer, with percentages calculated from zero-point energies and gas-phase partition functions in the standard way. It is easily seen that they correspond to the six structures derived from the C_2- and C_s-symmetric forms of the chain. The labels **a** and **b** are used to identify the structures with a synclinal (sharp) and an anticlinal (obtuse) dihedral angle [3][4] of the unit of the four consecutive atoms C(2′), C(1′), C(2), and N(1).

An interesting question concerns the height of the energetic barriers between the 14 conformers of the same set. Molecular models suggest that most conformers should readily undergo interconversion at room temperature. A quantitative assessment would require the computation of barrier heights between all conformers, which is not feasible with a sufficient precision at present. Experimental information on the minimal speed of interconversion can be obtained from the measurement of the ^{15}N-NMR spectrum. Room temperature measurements yield a single sharp line at −52.65 ppm, which establishes that barriers between the conformers of the same set are insufficient

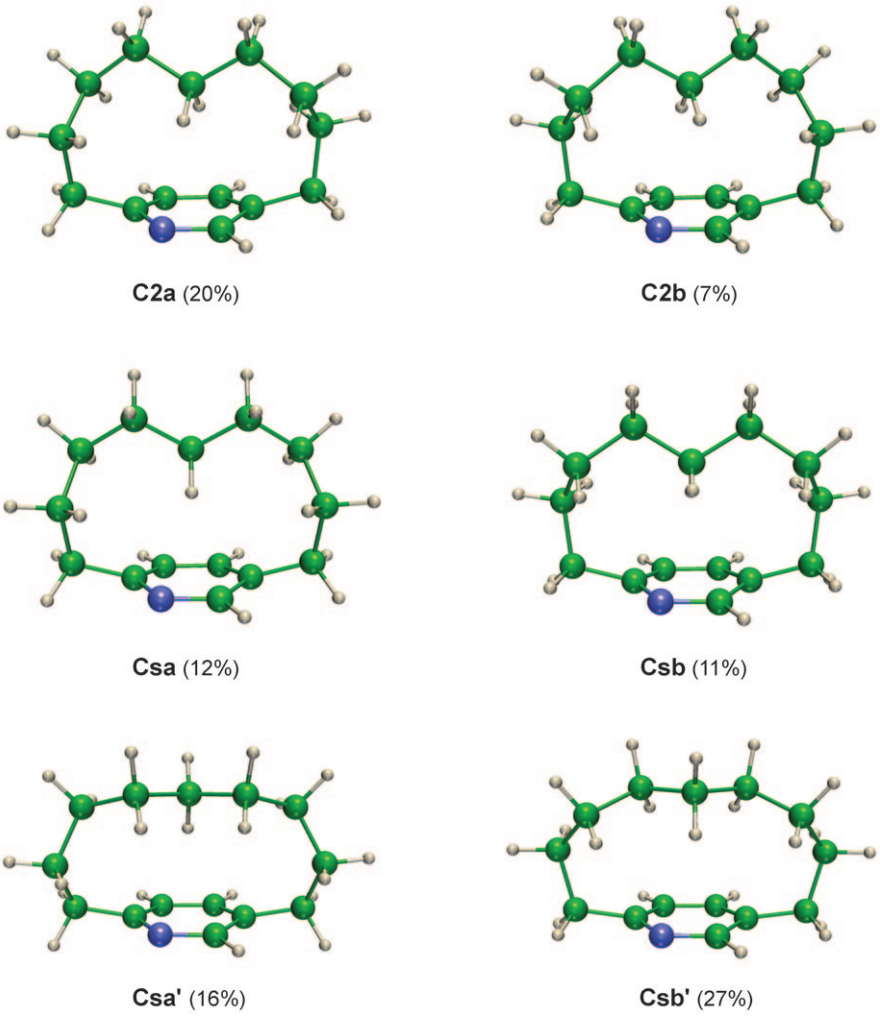

Fig. 1. *The six conformers of (*P*)-[9](2,5)pyridinophane with the lowest energy as computed by density-functional theory* (DFT) *with the B97-1 functional and the rpc-2 basis set.* The percentages are gas-phase values for 25°, and based on the harmonic approximation for zero-point vibrational energies and vibrational partition functions. The labeling of individual conformers is explained in the text.

to block interconversion. This finding agrees with the ^{13}C-NMR spectrum which exhibits only nine lines for the chain's nine CH_2 groups.

VOA of Individual Conformers. – The vibrations of [9](2,5)pyridinophane can be roughly divided into three groups: vibrations localized on the pyridine ring, vibrations localized on the $(CH_2)_9$ chain, and vibrations representing coupled motions of the nuclei of both fragments. Vibrations localized on the pyridine ring are similar for

different conformers and similar to those of nonchiral 2,5-substituted pyridines. Vibrations of the $(CH_2)_9$ chain, on the other hand, tend to depend on the particular geometry it assumes in different conformers.

Above 1500 cm^{-1}, VOA is due to motions of the pyridine moiety. In the range of 650 – 1500 cm^{-1}, it is generally dominated by motions of the $(CH_2)_9$ chain, more pronounced so for ROA than for VCD. This range cannot be subdivided into neat regions corresponding to rocking, twisting, wagging, and scissoring motions, even though many individual vibrations, such as the rocking vibrations calculated in the 680 to 750 cm^{-1} range, represent textbook examples of such classical shapes of motion. Rocking, mixed with twisting, can be found at higher energies, up to 950 cm^{-1}. Twisting motions span the range up to 1350 cm^{-1}, thus encompassing a region which is more characteristically associated with wagging motions. Characteristic wagging motions, in turn, occur from 1050 to 1400 cm^{-1}, coupled at lower energies with C – C bond stretching. Scissoring vibrations, in contrast, are calculated to occur distinct from other motions of the $(CH_2)_9$ chain, in the 1450 – 1500-cm^{-1} range.

The comparison of the individual ROA (*Fig. 2*) and the VCD (*Fig. 3*) spectra of the six conformers represented in *Fig. 1* provides unique insight into how the geometry of the $(CH_2)_9$ chain influences VOA. In the **C2a** and the **C2b** conformer, the chain represents a strongly chiral fragment with an opposite chirality sense for the two conformers. In the four **Cs**-type conformers, on the other hand, the chain itself is essentially achiral, and the overall chirality of the molecules derives from the presence of the N-atom in the pyridine ring. The VOA spectra reflect this: the spectra of **C2a** and **C2b** are large and essentially mirror images of each other, with a similarity of -0.84 for ROA and -0.55 for VCD, while those of **Csa** and **Csb**, and of **Csa′** and **Csb′**, are far smaller and not mirror-image-like (for the definition of similarity, see the *Exper. Part*). In the 650 – 1500-cm^{-1} region, the computed VOA of (–)-[9](2,5)pyridinophane is, therefore, largely determined by the difference in abundance of the **C2a** (20%) and **C2b** (7%) conformer.

It is instructive to compare the situation with 1,4-nonamethylenebenzene which has, except for the N-atom of the pyridine ring, the same structure as (–)-[9](2,5)pyridinophane. Its individual **Cs** and **Cs′** conformers are achiral and thus devoid of VOA, while the two chiral **C2** conformers have opposite and precisely cancelling VOA.

Characteristic Vibrations Localized on Fragments. – The precision of density-functional theory (DFT) calculations in rendering conformational equilibria is limited in the presence of intramolecular *Van der Waals* interactions. Such interactions are to be expected in (–)-[9](2,5)pyridinophane between the pyridine ring and the $(CH_2)_9$ chain. Moreover, the partition functions required in the calculation of relative abundances of conformers are evaluated for the gas phase, but VOA measurements need to be done in the condensed phase. This makes it imprudent to base the determination of the absolute conformation of this molecule on the overall appearance of computed VOA spectra, determined by the preponderance of conformation **C2a** over **C2b**. We will, therefore, compare here the VOA of two vibrations localized on the $(CH_2)_9$ chain, which tends to be characteristic of the variable geometry of the chain, with that of a vibration localized on the pyridine moiety, which has the same geometry in all conformers. In the subsequent section, we will see that the conclusions drawn on

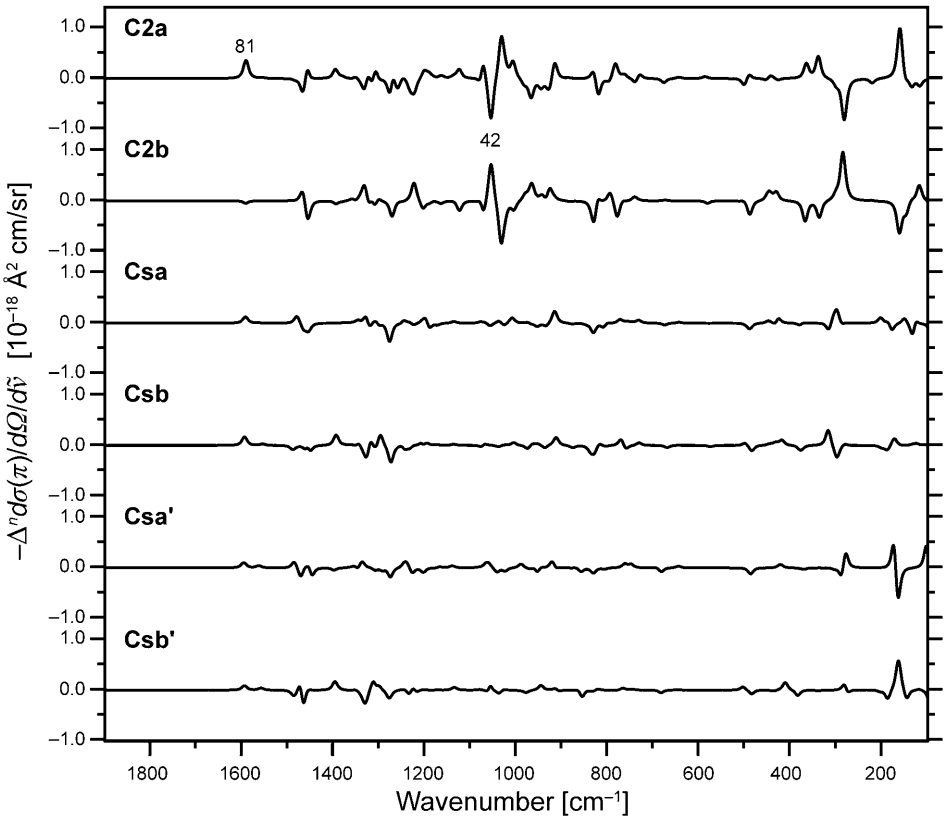

Fig. 2. *Computed* Raman *optical activity of the six lowest-energy conformers of* (P)*-[9](2,5)pyridinophane.* Calculation of geometries: DFT with the B97-1 functional and the rpc-2 basis set. Calculation of electronic tensors: time dependent *Hartree–Fock* theory with the rDPS basis set. Bands for individual vibrations were obtained by convoluting *Lorentzians* of 3.5-cm^{-1} full-width at half-maximum height (FWHM) for isotropic and 10 cm^{-1} for anisotropic scattering with an instrumental band shape assumed as a *Gaussian* of 7 cm^{-1} FWHM. The calculated frequencies were slightly shifted as explained in the *Exper. Part.*

the absolute conformations of the (−)-[9](2,5)pyridinophane molecule agree for both types of vibrations.

Raman Optical Activity (*ROA*). *Fig. 4* illustrates how ROA is generated in the conformers **C2a** and **C2b** of (−)-[9](2,5)pyridinophane by the ring stretching vibration 81, localized to 99% on the pyridine ring (fragment A), and by vibration 42, localized to the same extent on the $(CH_2)_9$ chain (fragment B). The measure for the localization is the distribution of the vibrational energy in the molecule.

Vibration 42, calculated at 1056 cm^{-1} for both conformers, is dominated by CH_2 wagging motions, with a C−C stretching component. It leads to a very strong negative ROA signal in **C2a**, and an equally strong positive signal in **C2b**. The group coupling matrices (GCM) [5] demonstrate that the ROA is indeed generated on the $(CH_2)_9$ chain (matrix element BB).

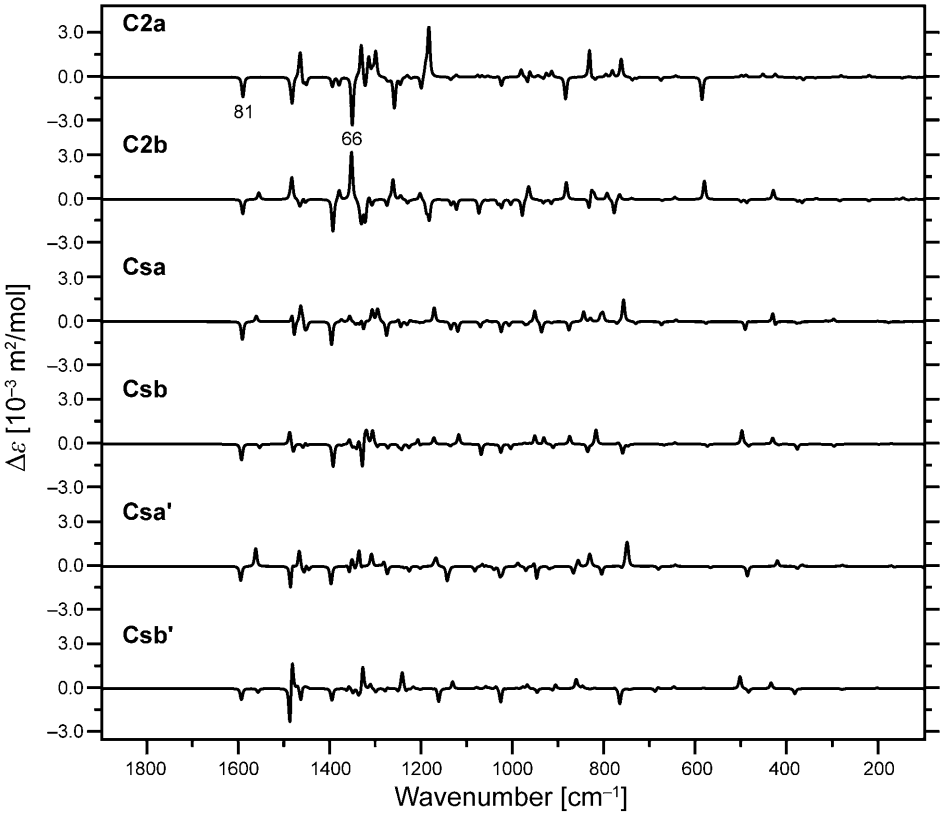

Fig. 3. *Computed vibrational circular dichroism of the six lowest-energy conformers of (*P*)-[9](2,5)pyridinophane.* Calculation of geometries and electronic tensors: DFT with the B97-1 functional and the rpc-2 basis set. Bands for individual vibrations were obtained by convoluting *Lorentzians* of 3.5-cm^{-1} FWHM with a *Gaussian* instrumental band shape of 4 cm^{-1}. The calculated frequencies were shifted as for *Fig. 2*.

Vibration 81, calculated at 1593 cm^{-1} for both conformers and observed at 1593 cm^{-1} in ROA and 1598 cm^{-1} in VCD[2]), is related to component a of the degenerate vibration 8 (*Wilson* notation) of benzene. Vibration 80, calculated at 1557 cm^{-1} and observed at 1562 cm^{-1}, corresponds to component b. In 2,5-dimetylpyridine, the two vibrations are observed at 1602 cm^{-1} and 1572 cm^{-1} [6], respectively. Vibration 81 stretches the pyridine ring in (–)-[9](2,5)pyridinophane in the 2–5 direction, while vibration 80 entails a motion, with an opposing sense for the C(2) and C(5), perpendicular to the line joining them. Only 81 leads to substantial ROA as well as VCD, and we will limit the discussion to it.

---

[2]) Other bands of characteristic vibrations show smaller wavenumber differences. Part of the discrepancy may be due to the differing envelopes of *Raman* and IR bands. *Raman* wavenumbers were verified to be precise within 1 cm^{-1}.

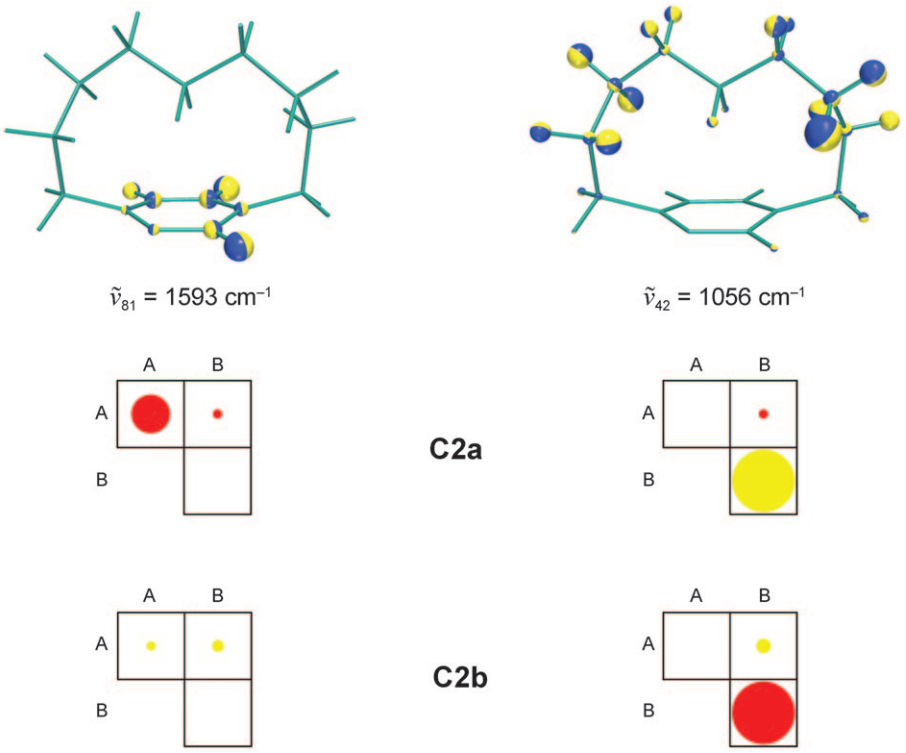

Fig. 4. *Comparison of the generation of ROA in conformer* **C2a** *and conformer* **C2b** *by vibrations 81 and 42, localized to 99% on the pyridine moiety* (group A), *and the* $(CH_2)_9$ *chain* (group B), *respectively.* The area of a circle in an element of a group coupling matrix (GCM) indicates the relative contribution to ROA generated within groups (elements AA and BB) and by their coupling (element AB). Red indicates a positive and yellow a negative contribution. For conformer **C2a**, the shape of the two vibrations is represented in the upper part of the drawing. The diameters of the spheres centered on the nuclei are proportional to their (classical) physical excursions, and the direction of motion is perpendicular to the plane separating the two differently colored halves of each sphere. The computational parameters are as in *Fig. 2*.

In conformer **C2a**, vibration 81 entails a small-to-medium-sized positive ROA effect, and, in conformer **C2b**, a negligibly weak negative one. The GCM in *Fig. 4* shows that the positive ROA of **C2a** is generated in the pyridine ring (element AA), and that little ROA is generated by either the chain, or coupling by the ring and chain (element AB).

The difference in the ROA produced by this strongly localized vibration in conformers **C2a** and **C2b** is neither due to a change in the vibration's shape, nor due to a change of the pyridine ring's geometry. The shape of the nuclear motions is identical for all **C2** and **Cs** conformers depicted in *Fig. 1*, with the similarity [7] on the pyridine fragment reaching an amazing 99.99%. The root-mean-square deviation (RMSD) of the equilibrium positions of the ring's nuclei amounts to a mere 0.003 Å. The reason for

the variation of the ROA must, therefore, lie with a through-space distortion of the ring's electron distribution by the proximity of the $(CH_2)_9$ chain.

This interpretation is supported by the positive ROA of vibration 81 in the four **Cs** conformers where the chains have an essentially achiral geometry. The GCMs depicted in *Fig. 5* are very similar, and the size of the elements AA is *ca.* half-way between that of **C2a** and **C2b**. This suggests that the bent pyridine ring, by itself, entails a positive ROA in vibration 81. This positive ROA appears amplified in conformer **C2a** through the distortion of the pyridine ring's electron distribution by the chiral $(CH_2)_9$ chain, but diminished in **C2b** where the chain has the opposite sense of chirality. The achiral chains of the four **Cs** conformers, on the other hand, seem to have no such effect.

Vibrational Circular Dichroism (*VCD*). The ring stretching vibration 81 yields moderately sized negative VCD for all the six main conformers, as evident from *Fig. 3*. The VCD GCMs [8] of the six conformers are similar, with those of **C2a** and **C2b** depicted in *Fig. 6*. It thus appears that the motion of the nuclei in the 2–5 direction of the bent pyridine ring in vibration 81 entails negative VCD, which depends little on the conformation of the $(CH_2)_9$ chain.

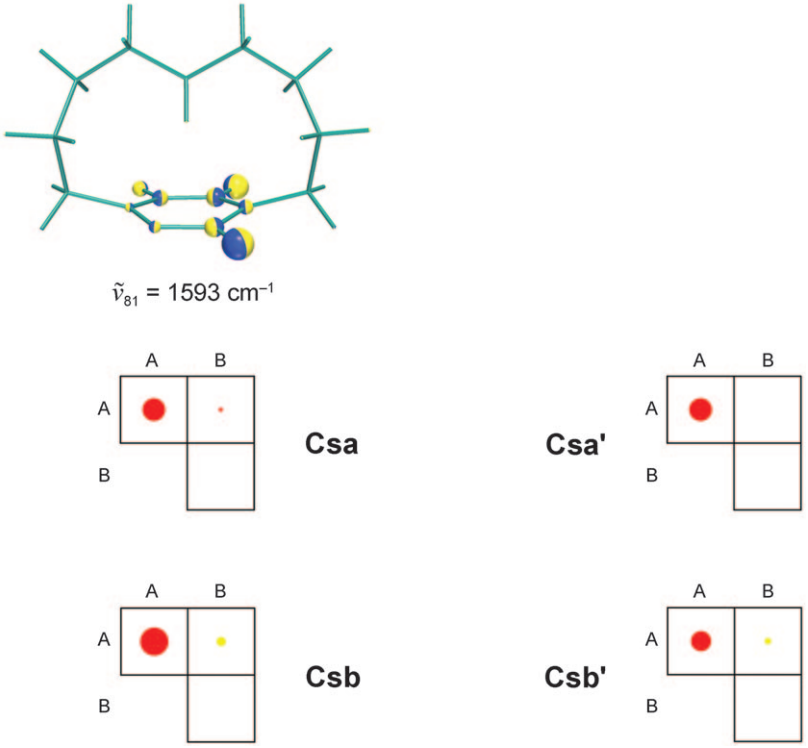

Fig. 5. *Shape of vibration 81 localized on the pyridine moiety for conformer* **Csa**, *and the ROA it generates in conformers* **Csa**, **Csb**, **Csa′**, *and* **Csb′**. For an explanation of the graphical representations, see *Fig. 4*. The computational parameters are as in *Fig. 2*.

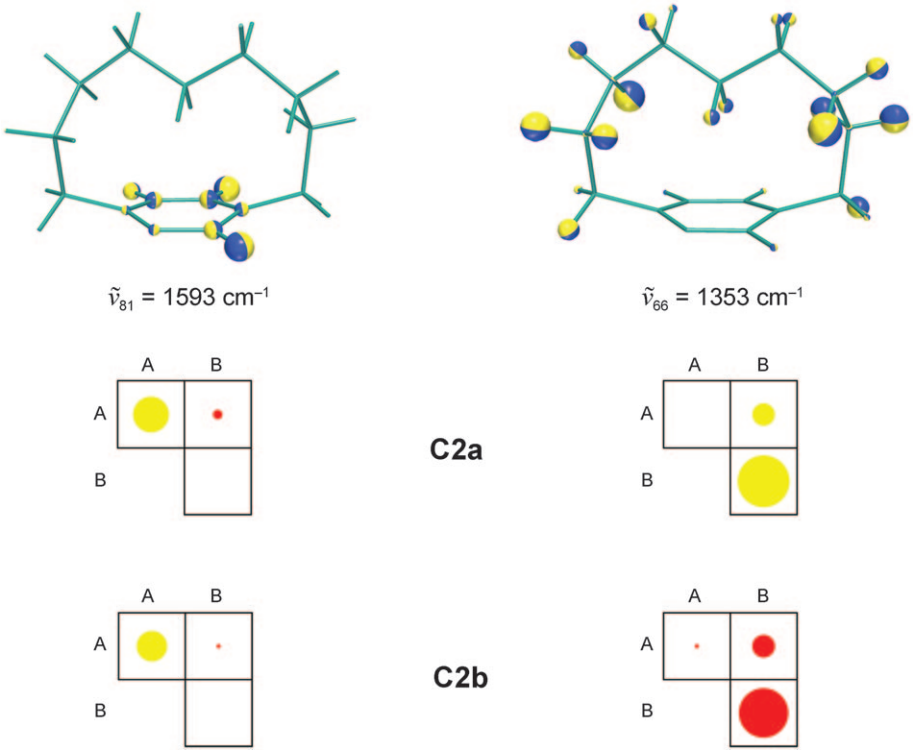

Fig. 6. *Comparison of the generation of VCD in conformer* **C2a** *and conformer* **C2b** *by vibrations 81 and 66, localized to 99% on the pyridine moiety* (group A) *and the* $(CH_2)_9$ *chain* (group B), *respectively.* The shape of the two vibrations is represented for conformer **C2a**. For an explanation of the graphical representations, see *Fig. 4*. The computational parameters are as in *Fig. 3*.

The behavior of the VCD of vibrations localized on the chain is similar to what was found for ROA, though not the same vibrations are of interest. The equivalent vibration in VCD to the wagging vibration 42 discussed for ROA is 66, despite the vibration's separation by 300 cm^{-1}. It represents a combination of wagging motions approximately antisymmetric with respect to the $(CH_2)_9$ chain's pseudo C_2-axis, while vibration 42 is approximately symmetric. Vibration 66 has pronounced VCD activity, similar to the ROA activity of 42. It is strongly negative in conformer **C2a** and positive in **C2b**, and thus characteristic of the geometry of the chains rather than the absolute conformation of the molecules, as found for the ROA of vibration 42.

Comparison of Measured and Computed VOA. – The ten conformers with the lowest energy make up, according to our *ab initio* computations, more than 99% of the equilibrium mixture at room temperature. They were all taken into account for comparing computed and experimental spectra, even though the bulk of the VOA is determined by the six conformers discussed in the previous sections. The VOA of the four conformers with the highest energy was not computed.

Fig. 7 shows the comparison of the computed and measured *Raman* and ROA spectra of (−)-[9](2,5)pyridinophane. The similarity reaches 0.65 for *Raman* and 0.35 for ROA. This suggests that the chirality sense of (−)-[9](2,5)pyridinophane is (*P*) as depicted in *Fig. 1*. For the opposite enantiomer, a value of −0.35 was obtained. The VCD spectra shown in *Fig. 8* confirm the chirality sense of (−)-[9](2,5)pyridinophane as (*P*), with values of 0.80 for the similarity of IR absorption and 0.47 for VCD.

Global values for similarity reflect the overall agreement or disagreement of spectra. For (−)-[9](2,5)pyridinophane, as explained in the previous section, the positive sign depends on the computational rendering of the predominance of conformer **C2a** over **C2b**. The similarity curves depicted in *Fig. 9* permit the inspection of spectral regions not determined by the $(CH_2)_9$ chain.

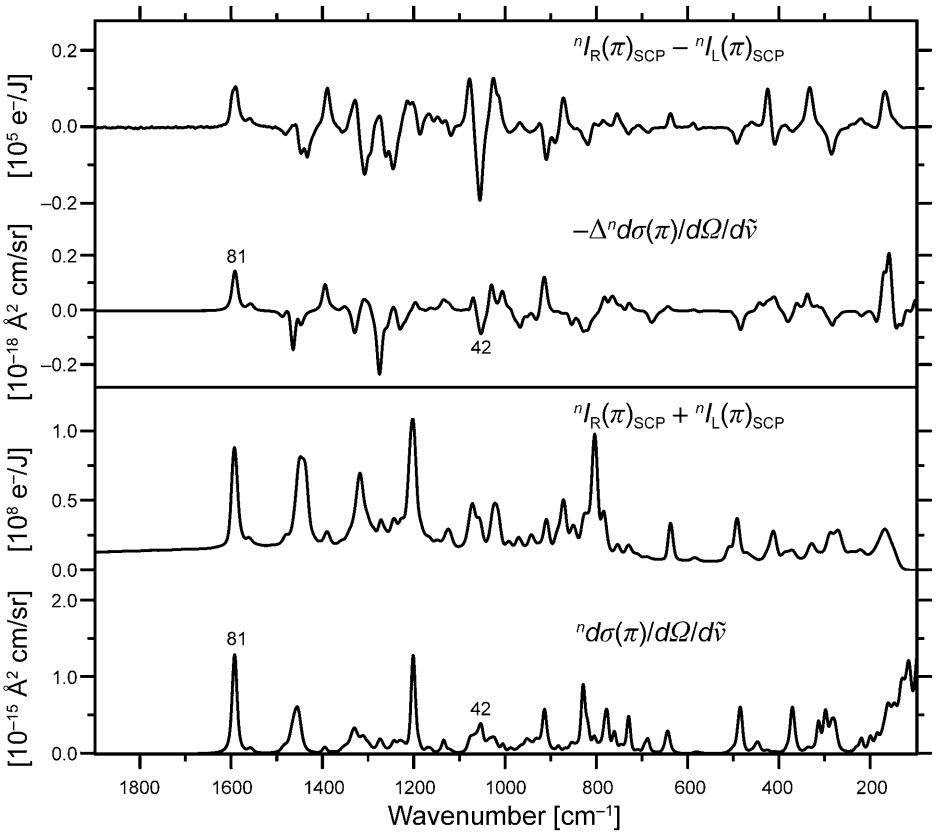

Fig. 7. *Experimental and computed ROA* (upper half) *and* Raman *scattering* (lower half). In each half, the top curve represents the experimental and the bottom curve the calculated spectrum. The ten lowest-energy conformers were included in the computation. The computational parameters are as in *Fig. 2*. Experimental parameters: exposure time: 60 min, laser power at sample: 200 mW, exciting wavelength: 532 nm, resolution: 7 cm^{-1}, sample size: 35 µl. The curves are slightly smoothed with a second-order *Savitzky–Golay* five-point procedure and represent detected photons per joule of exciting energy, per column of the charge coupled device detector, with one column covering 2.4 cm^{-1}.

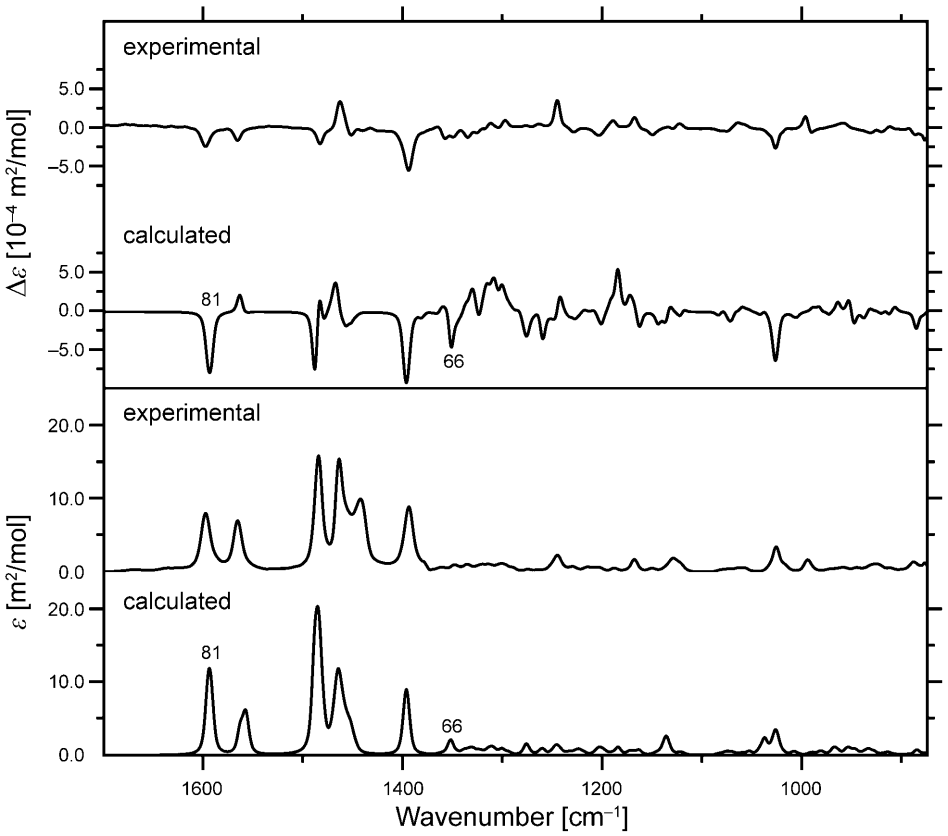

Fig. 8. *Experimental and computed VCD* (upper half)*, and IR absorption spectrum* (lower half). In each half, the top curve represents the experimental and the bottom curve the calculated spectrum. The ten lowest-energy conformers were included in the computation. The computational parameters are as in *Fig. 3*. The instrumental resolution was 4 cm^{-1}. For the low-absorbance regions, 20-min measurements were conducted with 100- and 50-μm path-length cells, and a 12-h measurement with a 6-μm path-length cell for precisely mapping the high-absorbance peaks in the 1300–1600 cm^{-1} region.

The curves show substantial positive peaks at 1593 cm^{-1} for ROA and 1598 cm^{-1} for VCD. The underlying spectral bands are due to the pyridine-ring stretching vibration 81 discussed in the preceding section. An even far larger positive peak occurs in VCD at 1398 cm^{-1}. It is due to vibration 69 calculated at 1396 cm^{-1}, with a moderately strong negative VCD effect for all conformers. This vibration is localized on the pyridine moiety, though not to the same extent as vibration 81, and related to vibration 19b of benzene. In ROA, it entails a positive sign which also leads to a sizable positive peak in the similarity curve. We notice that the degenerate vibration 19 of benzene is also at the root of a salient couplet observed at 1455 cm^{-1} in the first ROA spectra ever recorded over an extended wavenumber range [9].

Pyridine vibrations related to the degenerate benzene vibration 18 are likewise important in the 1040 cm^{-1} region where high positive similarity is found for VCD and

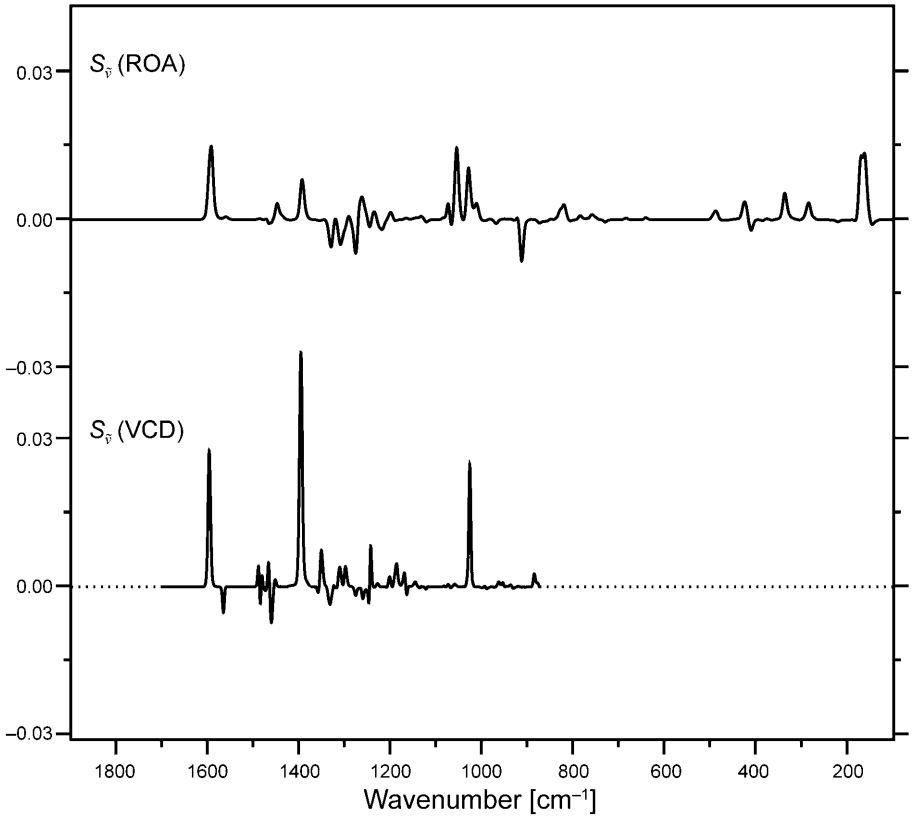

Fig. 9. *Similarity curves for the experimental and computed ROA* (top) *and VCD spectra* (bottom) *represented in* Figs. 7 *and* 8*, respectively.* Integrating the curves over the drawn wavenumber ranges yields the global similarities of 0.35 for ROA and 0.47 for VCD.

ROA, but the unequivocal attribution to experimental bands is difficult for ROA. Overall, the VOA of vibrations localized on the pyridine moiety provides solid confirmation for the absolute conformations of the (–)-[9](2,5)pyridinophane molecule to be (*P*), as suggested by the overall appearance of VOA spectra.

Conclusions. – The *CIP* descriptor (*P*) applies to the (–)-enantiomer of [9](2,5)pyridinophane with individual conformers indicated in *Fig. 1*. It can be assigned unequivocally by the VOA of bands due to vibrations localized on the nonplanar pyridine moiety of the molecule, with VCD supporting conclusions originally reached by ROA alone. The measurements were performed with a newly resolved sample with a 90.5% enantiomeric excess, as determined by NMR with a chiral europium shift reagent.

The computational part of the work was compounded by the unexpectedly large number of conformers of [9](2,5)pyridinophane. They fall into two enantiomorphic sets

which do not undergo interconversion up to a temperature of 250°. According to our calculations, each set comprises 14 individual conformers, six of which make up more than 90% of a set's equilibrium mixture at room temperature. ^{15}N-NMR Spectra show that the conformers of the same set, which stem from the different geometries which the $(CH_2)_9$ chain can assume, undergo interconversion rapidly at room temperature.

The experimental ROA spectrum extends over a larger spectral range than the VCD spectrum. Even for the same spectral range, the ROA spectrum appears somewhat more structured, with more bands of a comparable size, than the VCD spectrum. In the computed spectra of individual conformers, the region with the largest bands occurs at wavenumbers by *ca.* 300 cm^{-1} higher in VCD than in ROA. At wavenumbers below 700 cm^{-1}, computed VCD is strikingly lower than ROA. Due to experimental constraints, experimental VCD cannot be measured in this spectral range, but the expected small size of signals does not make this a limitation to the practical usefulness of VCD.

The similarity between measured and computed spectra is higher for VCD than for ROA. The precision of the measured ROA data is not at the root of this [10]. The same force field was used for the calculation of VCD and ROA. The lower value of the similarity for ROA must, therefore, be attributed either to a lower quality of the electronic tensor calculation, and/or to the fact that the vibrations which carry large VCD are not identical to those which carry large ROA. The higher weight in ROA of vibrations localized mainly on the $(CH_2)_9$ chain, and also of vibrations extending over the pyridine moiety and the chain, concurs with the idea that the nature of vibrations matters. The net contribution to observed VOA by such vibrations depends on the correct computational rendering of the abundance of conformers, which is expected to be limited in a DFT calculation of a molecule with strong intramolecular *Van der Waals* interactions. (−)-[9](2,5)pyridinophane is, therefore, an interesting test case for recent functionals claimed to better account for this kind of interaction in DFT calculations [11].

The authors are grateful to *R. Lombardi* and Prof. *L. A. Nafie* for the measurement of the VCD spectra, and to Prof. *B. Wrackmeyer* from the University of Bayreuth for the ^{15}N-NMR data and computational information on one of the difficult to identify conformers. Prof. *K.-H. Seifert* and Mr. *T. Müller* helped to isolate and characterize the (−)-enantiomer. Mr. *P. Oulevey* calculated the **Csa′** and **Csb′** conformers, and Dr. *J. Cheeseman* from *Gaussian Inc.*, Wallingford, Connecticut, USA, verified the validity of the convergence of the DFT calculations of two conformers with a new release version of the *Gaussian* program suite. Particular thanks go to the *Centre for Theoretical Computational Chemistry* (*CTCC*) and the *University of Tromsø* for giving access to their supercomputer resources. The work was supported through the *Swiss National Science Foundation* grants 200020-112201 and 200020 – 120142/1.

Experimental Part

Resolution of [9](2,5)Pyridinophane. To a boiling soln. of 4.00 g (10.7 mmol) of (−)-2,2′-dihydroxy-1,1′-binaphtyl-3,3′-dicarboxylic acid [12] in 40 ml of EtOH, 4.43 g (21.4 mmol) racemic [9](2,5)pyridinophane [1] were added. After 15 h at r.t., the crystals, which had formed, were separated and recrystallized form 100 ml of EtOH. The crystals formed (3.4 g) were dissolved in 2N NaOH and extracted with $CHCl_3$. Removal of the solvent yielded 1.15 g (30%) of (−)-[9](2,5)pyridinophane, b.p. 80°/0.01 Torr, $[\alpha]_D^{25} = -156.0$ ($c = 2.28$, cyclohexane). The ^{1}H-NMR ($CDCl_3$) spectrum was identical with that of the racemic compound [1]. Addition of 0.4 equiv. of the chiral shift reagent tris{3-

[(heptafluoropropyl)(hydroxy)methylene]-*d*-camphorato}europium(III) ([Eu(hfc)$_3$]; *Fluka*) gave separate signals for H–C(6) in a 1.00 : 0.05 ratio, indicating a 90.5% enantiomeric excess (ee).

The mother liquor of the first crystallization yielded (+)-[9](2,5)pyridinophane with $[\alpha]_D^{25} = +102.4$ ($c = 3.68$, cyclohexane). The ^{1}H-NMR ($CDCl_3$) spectrum with added shift reagent [Eu(hfc)$_3$] gave separate signals for H–C(6) in a 0.255 : 1.00 ratio, corresponding to a 59.5% enantiomeric excess. The values obtained for the (+)- and (−)-sample thus led to the same specific rotation $[\alpha]_D^{25} = +/-172$ for the pure enantiomers of [9](2,5)pyridinophane.

Measurements. Optical rotations were measured with a *Perkin-Elmer 297* spectropolarimeter. ^{1}H- and ^{13}C-NMR measurements (^{1}H: 300 and ^{13}C: 75.5 MHz) were performed with a *Bruker AC-300*, and the ^{15}N-NMR (40.5 MHz) with a *Varian INOVA-400* spectrometer. *Raman* and ROA spectra were recorded with an instrument constructed at the University of Fribourg [13] with technical details as described in [10] and [14]. IR and VCD measurements were carried out with a standard dual source *Chiral IR* VCD spectrometer from *BioTools, Inc.* (Jupiter, Florida, USA) equipped with a *Dual PEM* accessory [15].

Computations. Geometries and force fields were calculated with the Gaussian program suite [16] with DFT, the B97-1 functional [17], and the rpc-2 [7][18] basis set derived from the pc-2 set [19]. The same approach was used for IR and VCD with the *Dalton* program [20]. The electronic tensors for *Raman* and ROA were calculated with the *Dalton* program with time dependent *Hartree–Fock* theory and the rDPS basis set [21]. The frequencies calculated in the harmonic approximation were multiplied with a factor linearly dependent on wavenumbers, set to 0.98 at 1600 cm^{-1} and 1.00 at 300 cm^{-1} in order to maximize overlap of computed and measured bands for evaluating the similarity of spectra. Quoted values are the corrected frequencies.

The similarity curve $S_{ab}(\tilde{\nu})$ for two spectra a and b is obtained as

$$S_{ab}(\tilde{\nu}) = \frac{I_a(\tilde{\nu}) I_b(\tilde{\nu})}{\sqrt{\int_{\tilde{\nu}=\tilde{\nu}_1}^{\tilde{\nu}_2} I_a(\tilde{\nu}) I_a(\tilde{\nu}) \int_{\tilde{\nu}=\tilde{\nu}_1}^{\tilde{\nu}_2} I_b(\tilde{\nu}) I_b(\tilde{\nu})}}$$

where $I_a(\tilde{\nu})$ and $I_b(\tilde{\nu})$ are spectral intensities as a function of the wavenumber $\tilde{\nu}$. In practice, integration is replaced by a summation over discrete spectral intervals chosen as 1/7 of a wavenumber.

Vibrational motions were analyzed, and group coupling matrices (GCMs) and spectral similarities computed, with PyVib2 [22].

REFERENCES

[1] H. Gerlach, E. Huber, *Helv. Chim. Acta* **1968**, *51*, 2027.
[2] J. Haesler, I. Schindelholz, E. Riguet, C. G. Bochet, W. Hug, *Nature* **2007**, *446*, 526.
[3] W. Klyne, V. Prelog, *Experientia* **1960**, *16*, 521.
[4] V. Prelog, G. Helmchen, *Angew. Chem., Int. Ed.* **1982**, *21*, 567.
[5] W. Hug, *Chem. Phys.* **2001**, *264*, 53.
[6] F. R. Dollish, W. G. Fateley, F. F. Bentley, 'Characteristic Raman Frequencies of Organic Compounds', John Wiley & Sons, New York, 1974.
[7] W. Hug, M. Fedorovsky, *Theor. Chem. Acc.* **2008**, *119*, 113.
[8] W. Hug, J. Haesler, *Int. J. Quantum Chem.* **2005**, *104*, 695.
[9] W. Hug, S. Kint, G. F. Bailey, J. R. Scherer, *J. Am. Chem. Soc.* **1975**, *97*, 5589; W. Hug, A. Kamatari, K. Srinivasan, H.-J. Hansen, H.-R. Sliwka, *Chem. Phys. Lett.* **1980**, *76*, 469.
[10] W. Hug, *Appl. Spectrosc.* **2003**, *57*, 1.
[11] P. Oulevey, W. Hug, unpublished work.
[12] K. Weil, W. Kuhn, *Helv. Chim. Acta* **1944**, *27*, 1648.
[13] J. Haesler, Ph.D. Thesis, University of Fribourg, 2006.
[14] W. Hug, G. Hangartner, *J. Raman Spectrosc.* **1999**, *30*, 841.

[15] L. A. Nafie, *Appl. Spectrosc.* **2000**, *54*, 1634; L. A. Nafie, R. K. Dukor, T. B. Freedman, in 'Handbook of Vibrational Spectroscopy', Eds. J. M. Chalmers, P. R. Griffits, John Wiley and Sons, Chichester, 2002, Vol. 1, p. 731; L. A. Nafie, H. Buijs, A. Rilling, X. Cao, R. K. Dukor, *Appl. Spectrosc.* **2004**, *58*, 647.
[16] M. J. Frisch, Gaussian 03 Revision E.01, *Gaussian Inc.*, 2004.
[17] F. A. Hamprecht, A. J. Cohen, D. J. Tozer, N. C. Handy, *J. Chem. Phys.* **1998**, *109*, 6264.
[18] M. Fedorovsky, Ph.D. Thesis, University of Fribourg, 2008.
[19] F. Jensen, *J. Chem. Phys.* **2001**, *115*, 9113.
[20] DALTON, A Molecular Electronic Structure Program Release 2.0, http://www.kjemi.uio.no/software/dalton/dalton.html, 2005.
[21] G. Zuber, W. Hug, *J. Phys. Chem. A* **2004**, *108*, 2108.
[22] M. Fedorovsky, PyVib2, A Program for Analyzing Vibrational Motion and Vibrational Spectra, http://pyvib2.sourceforge.net, 2007; M. Fedorovsky, *Comput. Lett.* **2006**, *2*, 233.

Received January 23, 2009